

Nonlocal response of a small coated sphere

R. Rojas and F. Claro

*Solid State Division, Oak Ridge National Laboratory, Oak Ridge, Tennessee 37831
and Department of Physics, University of Tennessee, Knoxville, Tennessee 37916*

R. Fuchs

Ames Laboratory and Iowa State University, Ames, Iowa 50011

(Received 10 December 1986; revised manuscript received 9 November 1987)

A theory for the response of a small spherical particle with a coating is developed using the semiclassical infinite-barrier model. Both the core and the outer layer are described by a nonlocal dielectric function. The theory is applied to an Al_2O_3 -coated Al sphere and to an Sn-coated Al_2O_3 sphere, and we find the coating to dominate the high-multipole response of the particle in either case. The optical-absorption and scanning tunneling electron microscopy spectra of the above systems are discussed.

I. INTRODUCTION

The interaction between a spherical particle and electromagnetic radiation was first treated in the pioneering work of Mie.¹ This classical solution has been extensively used in the analysis of systems of small, well-separated metal particles with diameters greater than about 30 Å. In principle, optical measurements in such systems provide a useful test of the theory but there are experimental difficulties to produce samples with such ideal characteristics as equally separated particles, spherical form and unique radius, absence of oxide coatings over the metallic core, etc. More recent techniques that use the scanning transmission electron microscope (STEM) test the response of individual particles by measuring the energy distribution of the scattered electrons.² Experiments done on single spheres show the accuracy of predictions of the Mie theory.³ Results for two spheres also show the importance of couplings of high-pole order between the particles, as predicted recently.^{4,5} Detailed interpretation of experimental results has not always been possible however and more theoretical work that treats the effect of clustering, oxide overlayers and nonlocal effects in the metal is needed in order to get quantitative agreement.⁶

The importance of an oxide overlayer on the far-infrared response of a metal sphere has been recognized since the work of Weaver *et al.*⁷⁻¹⁵ The oxide has a resonance in this region that is expected to produce at least as much absorption as the metal. Also, recent work shows the importance of nonlocal effects in explaining experiments on photoemission.¹⁶⁻²² A nonlocal dielectric function couples the surface excitations to bulk-plasmon modes and may provide additional interaction mechanisms through the creation of electron-hole pairs. Nonlocal results for the polarizabilities of arbitrary pole order using the hydrodynamical model and the Lindhard-Mermin dielectric function were recently reported.²³ A cutoff on excitations of high order is provided by the nonlocal nature of the dielectric function. A similar effect has been found in the quantum limit of very small spheres.²⁴

In the present work we study the nonlocal response to an electromagnetic excitation of a small coated sphere. The cases of oxide over metal as well as metal over oxide are discussed. We are interested in the coupling of the particle with the electric field and ignore magnetic effects. The first case has been previously treated by several authors using a local dielectric function.⁷⁻¹¹ The motivation has been the understanding of the anomalous low-frequency absorption obtained in optical experiments and most work is concerned with this region of the spectrum. In this paper we discuss the multipolar response of the nonlocal coated particle in a wide frequency range that includes the plasma frequency of the metal and higher. Our main finding is that the coating, no matter how thin it is, dominates the response at high polar order. The paper is organized as follows. In Sec. II a theory of the electric polarizability of a sphere with one or more overlayers is developed using the semiclassical infinite-barrier (SCIB) model and the response of an oxide-over-metal as well as metal-over-oxide sphere is discussed. In Sec. III the theory is used to obtain the optical absorption of an aluminum-oxide-coated aluminum core, as well as a tin-coated aluminum-oxide core. Section IV treats the loss of a charged particle moving uniformly past a sphere, and finally in Sec. V our conclusions are presented.

II. NONLOCAL POLARIZABILITIES

We begin by considering an uncoated sphere of radius a composed of a material characterized by a nonlocal bulk dielectric function $\epsilon_a(k, \omega)$, surrounded by a homogeneous medium with a local dielectric function $\epsilon_h(\omega)$. We assume our sphere is under the influence of an external potential

$$V^{\text{ext}}(\mathbf{r}) = V_l r^l P_l(\cos\theta), \quad (1)$$

where $\mathbf{r} = (r, \theta, \phi)$ are spherical coordinates whose origin is at the sphere center, P_l is a Legendre polynomial of order l , and V_l is a constant. This applied potential excites in the sphere the multipole q_l

$$q_l = -\frac{2l+1}{4\pi} \alpha_l V_l, \quad (2)$$

where α_l is the l -polar polarizability.²⁵ A potential

$$V^{\text{ind}}(\mathbf{r}) = -\alpha_l V_l \frac{P_l(\cos\theta)}{r^{l+1}} \quad (3)$$

is induced in the region $r \geq a$. In order to get α_l , we solve the electrostatic equations with the usual boundary conditions on the sphere surface: (i) continuity of the potential, and (ii) continuity of the normal component of the displacement vector. Outside the sphere we solve Laplace's equation by simply adding the external and induced potentials,

$$V(\mathbf{r}) = V_l \left[r^l - \frac{\alpha_l}{r^{l+1}} \right] P_l(\cos\theta). \quad (4)$$

The radial component of the corresponding displacement vector \mathbf{D} is

$$D_r = -\epsilon_h V_l \left[l r^{l-1} + (l+1) \frac{\alpha_l}{r^{l+2}} \right] P_l(\cos\theta), \quad (5)$$

where we took advantage of the local dielectric properties of the medium surrounding the sphere. We next define the surface impedance

$$Z_a = \frac{V(a)}{a D_r(a)}, \quad (6)$$

a quantity that will prove to be useful, especially in the case of a coated sphere because both quantities in definition (6) are continuous through the spherical boundary and can be evaluated by using solutions at either side. The following expression relating Z_a to the l -polar polarizability is obtained by inserting the external solution ($r \geq a$) given by Eqs. (4) and (5) into definition (6):

$$Z_a = \frac{\alpha_l - a^{2l+1}}{\epsilon_h [l a^{2l+1} + (l+1) \alpha_l]}. \quad (7)$$

Inside the sphere we have to solve the electrostatic equations

$$\nabla \cdot \mathbf{D} = 0, \quad (8a)$$

$$\nabla \times \mathbf{E} = 0, \quad (8b)$$

with the field intensity \mathbf{E} and the displacement \mathbf{D} being related through the nonlocal relation

$$\mathbf{D}(\mathbf{r}) = \int \epsilon_a(\mathbf{r}-\mathbf{r}', \omega) \mathbf{E}(\mathbf{r}') d^3 r'. \quad (8c)$$

To get the solution inside we use the semiclassical infinite barrier (SCIB) model whose prescription is as follows:^{26,27} extend the nonlocal response to all space, and solve in an unbounded medium a Poisson-type equation for a potential function $V_D(\mathbf{r})$ defined by

$$-\nabla V_D(\mathbf{r}) = \mathbf{D}(\mathbf{r}), \quad (9)$$

with charge sources of the appropriate symmetry located on the sphere surface. Then, the equation to solve is

$$\nabla^2 V_D(\mathbf{r}) = C_l \delta(r-a) Y_{l0}(\theta, \phi), \quad (10)$$

where $P_l(\cos\theta)$ has been replaced by its corresponding expression in terms of $Y_{l0}(\theta, \phi)$ and C_l stands for an unknown l -dependent constant. Equation (10) is solved by first taking its Fourier transform

$$-k^2 V_D(\mathbf{k}) = C_l \int \delta(r-a) Y_{l0}(\theta, \phi) e^{-i\mathbf{k}\cdot\mathbf{r}} d^3 r, \quad (11)$$

and next by expanding the exponential in terms of spherical Bessel functions and spherical harmonics. Using the orthogonality relation of the latter we obtain the solution in wave-vector space

$$V_D(\mathbf{k}) = -\frac{4\pi a^2}{k^2} C_l (-i)^l j_l(ka) Y_{l0}(\theta_k, \phi_k), \quad (12)$$

where we have used the notation $\mathbf{k} = (k, \theta_k, \phi_k)$. By taking the inverse Fourier transform of the above equation we obtain

$$V_D(\mathbf{r}) = -\frac{2}{\pi} a^2 C_l Y_{l0}(\theta, \phi) \int_0^\infty j_l(ka) j_l(kr) dk. \quad (13)$$

Using the formula²⁸

$$\int_0^\infty j_l(\alpha x) j_l(\beta x) dx = \frac{\pi}{2} \frac{1}{2l+1} \frac{\alpha^l}{\beta^{l+1}}, \quad \beta > \alpha \quad (14)$$

we finally get

$$V_D(\mathbf{r}) = -\frac{C_l}{2l+1} Y_{l0}(\theta, \phi) \frac{r^l}{a^{l-1}}, \quad r < a. \quad (15)$$

This result has the usual coordinate dependence of Laplace's solutions inside a spherical volume. This could have been guessed at first because the charge sources of the potential V_D are on the surface of the spherical volume. The solution for the true potential $V(\mathbf{r})$ inside the sphere is obtained through the relation

$$V_D(\mathbf{k}) = \epsilon_a(\mathbf{k}, \omega) V(\mathbf{k}). \quad (16)$$

Proceeding as with Eq. (12) and assuming the \mathbf{k} dependence of $\epsilon_a(k, \omega)$ to be isotropic, the electric potential inside the sphere is then given by

$$V(r) = -\frac{2}{\pi} a^2 C_l Y_{l0}(\theta, \phi) \int_0^\infty \frac{j_l(ka) j_l(kr)}{\epsilon_a(k, \omega)} dk, \quad r < a. \quad (17)$$

The vector fields \mathbf{E} and \mathbf{D} inside the sphere are obtained through the relations

$$\mathbf{E} = -\nabla V, \quad (18a)$$

$$\mathbf{D} = -\nabla V_D. \quad (18b)$$

The final step is the matching of the internal and external solutions through the boundary conditions on the sphere surface. Two equations are thus obtained and they yield the values

$$C_l = -(2l+1)a^{l-1} \left[1 + \frac{l+1}{l} \left[\frac{\alpha_l}{a^{2l+1}} \right] \right] \epsilon_h V_l, \quad (19a)$$

$$\alpha_l = \frac{l(E_l - \epsilon_h)}{l(E_l + \epsilon_h) + \epsilon_h} a^{2l+1}, \quad (19b)$$

where

$$E_l = E_l(\omega) = \left[\frac{2}{\pi} (2l+1)a \int_0^\infty \frac{j_l^2(ka)}{\epsilon_a(k, \omega)} dk \right]^{-1}. \quad (20)$$

As is apparent in Eq. (19b), the quantity E_l has the role of an effective l -dependent dielectric constant for the bulk material of the sphere. In the local limit of a k -independent dielectric function one has $E_l(\omega) = \epsilon_a(\omega)$ and Eq. (19b) assumes its usual form.²⁹ The result (19b) was obtained previously for the case $\epsilon_h = 1$ by Fuchs and Claro.²³ Form (20) for the dielectric constant describes the response of a medium in a basis of excitations of spherical symmetry. Introducing the result (19b) in Eq. (7) we further get the simplest expression

$$Z_a = -\frac{1}{lE_l}. \quad (21)$$

Now we assume that a coating of material characterized by a nonlocal dielectric function $\epsilon_b(k, \omega)$ and thickness t is added to the sphere. The procedure to get the sphere l -polar polarizabilities is similar to the previous one. The analysis of the external solution is just the same so we just get Eq. (7) in the form

$$Z_b = \frac{\alpha_l - b^{2l+1}}{\epsilon_h [lb^{2l+1} + (l+1)\alpha_l]}, \quad (22)$$

where α_l is the coated-sphere polarizability and $b = a + t$ is the new radius. The previous analysis of the internal solution is also valid here and the results given by Eqs. (20) and (21) for E_l and Z_a , respectively, are the same without change. Naturally, Eqs. such as (19a) and (19b) that depend on the matching of solutions at the surface $r = a$ are not valid here, and we have to solve the electrostatic equations in the coating region ($a \leq r \leq b$) to make a new matching with the previously found solutions. Indeed, to get the sphere polarizabilities we only need a relation between Z_a and Z_b , which together with Eqs. (20), (21), and (22) will give us the desired α_l . Getting Z_b in terms of Z_a is almost equivalent to solving completely the electrostatic problem in the coating region, and we proceed once again by following the SCIB prescription. We add source charges of the potential V_D on the surfaces at $r = a$ and $r = b$, we extend to infinity and to the

origin the coating medium and we solve the equation

$$\nabla^2 V_D(\mathbf{r}) = [A_l \delta(r-a) + B_l \delta(r-b)] Y_{l0}(\theta, \phi). \quad (23)$$

A similar procedure to that followed in the case of an uncoated sphere leads to the following potentials $V_D(\mathbf{r})$ and $V(\mathbf{r})$:

$$V_D(\mathbf{r}) = -\frac{1}{2l+1} \left[A_l a^2 \frac{a^l}{r^{l+1}} + B_l b^2 \frac{r^l}{b^{l+1}} \right] Y_{l0}(\theta, \phi), \quad (24a)$$

$$V(\mathbf{r}) = -\frac{2}{\pi} a^2 Y_{l0}(\theta, \phi) \times \int_0^\infty j_l(kr) \left[\frac{A_l j_l(ka) + B_l j_l(kb)}{\epsilon_b(k, \omega)} \right] dk, \quad (24b)$$

both results being valid in the region $a \leq r \leq b$. The unknown constants A_l , B_l , C_l , and α_l could be found by matching the solutions at surfaces $r = a$ and $r = b$, but in order to obtain α_l only, we follow a different procedure. We first get the surface impedance by use of the results (24a) and (24b) together with Eq. (18b) in the definition (6),

$$Z_a = \frac{F_{ab} + F_a \left[\frac{a}{b} \right]^{l-1} \frac{B_l}{A_l}}{F_a F_{ab} \left[l+1-l \left[\frac{a}{b} \right]^{l-1} \frac{B_l}{A_l} \right]}, \quad (25a)$$

$$Z_b = \frac{F_b + F_{ab} \left[\frac{b}{a} \right]^{l+2} \frac{B_l}{A_l}}{F_b F_{ab} \left[l+1-l \left[\frac{b}{a} \right]^{l+2} \frac{B_l}{A_l} \right]}. \quad (25b)$$

Here $F_a = E_l^b(a, a)$, $F_b = E_l^b(b, b)$, and $F_{ab} = E_l^b(a, b)$, where

$$E_l^x(p, q) = \left[\frac{2}{\pi} (2l+1) \left[\frac{q}{p} \right]^l q \int_0^\infty \frac{j_l(kp) j_l(kq)}{\epsilon_x(k, \omega)} dk \right]^{-1}, \quad p \leq q \quad (26)$$

where x can be either a or b . Notice that our former E_l of Eq. (20) is given here by $E_l = E_l^a(a, a)$. The desired relation between impedances Z_a and Z_b is obtained by eliminating the ratio B_l/A_l between Eqs. (25a) and (25b). The result is

$$Z_b = \frac{(l+1)F_a F_{ab} Z_a - F_{ab} + F_a F_b (F_{ab}^{-1} + l Z_a)(a/b)^{2l+1}}{F_a F_b F_{ab} [l F_a^{-1} - l(l+1)Z_a + (l+1)(F_{ab}^{-1} + l Z_a)](a/b)^{2l+1}}. \quad (27)$$

Finally, by combining relations (21), (22), and (27) we get the l -polar polarizabilities of a coated sphere characterized by two nonlocal dielectric functions $\epsilon_a(k, \omega)$ and $\epsilon_b(k, \omega)$, corresponding to the core and coating, respectively:

$$\alpha_l = b^{2l+1} \frac{F_{ab}(1 - \epsilon_h/F_b)[lE_l + (l+1)F_a] + F_a[(l+1)(E_l - F_{ab}) + l\epsilon_h(E_l/F_{ab} - 1)](a/b)^{2l+1}}{F_{ab}[1 + (l+1)\epsilon_h/F_b][lE_l + (l+1)F_a] + F_a(l+1)(\epsilon_h + E_l - F_{ab} - \epsilon_h E_l/F_{ab})(a/b)^{2l+1}}. \quad (28)$$

For k -independent dielectric functions we have $F_a = F_b = F_{ab} = \epsilon_b(\omega)$, $E_l = \epsilon_a(\omega)$ and the previous expression is reduced to its local version.³⁰

The procedure followed here to find the polarizability of a coated sphere can be extended to an arbitrary number of coats by using repeatedly the impedance transfer relation (27) together with Eqs. (21) and (22).

The electric polarizability (28) exhibits an interesting behavior in the limit when l is large enough so that $(a/b)^{2l+1} \ll 1$. In that case we get the approximate local relation

$$\alpha_l = b^{2l+1} \frac{\epsilon_b - \epsilon_h}{\epsilon_b + \frac{l+1}{l} \epsilon_h}, \quad (29)$$

a result that is independent of the core dielectric function. Comparing this expression with (19b) we see that

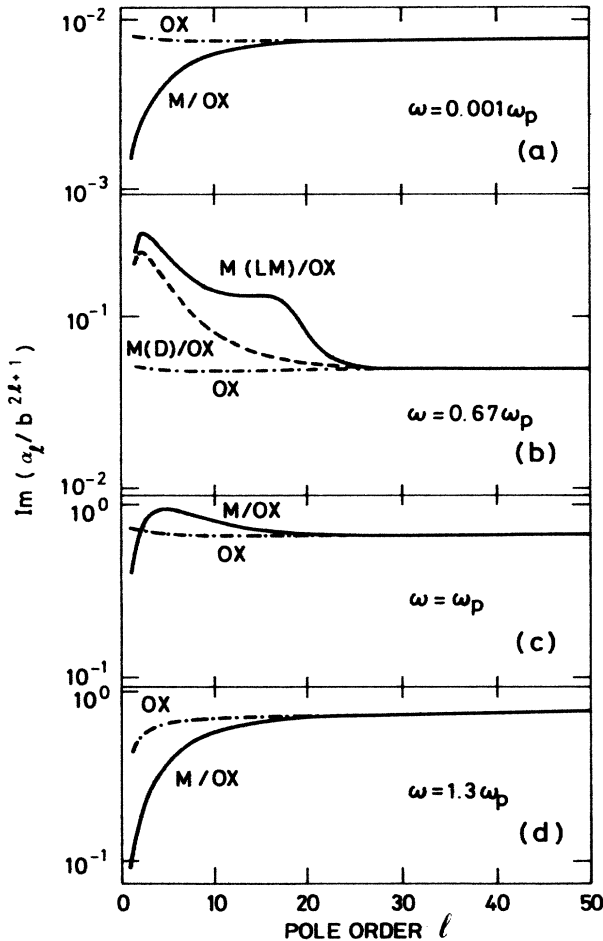


FIG. 1. Imaginary part of the l -pole polarizability of an oxide-coated Al sphere at various frequencies. The metallic (M) core is 100 Å in diameter and the Al₂O₃ (OX) coating is 5 Å thick. Expression (30) was used for the dielectric function of the oxide. Both a Lindhard-Mermin (LM) and a Drude (D) dielectric function were used for the metal and the results are different only in case (b). The polarizabilities of a pure oxide sphere 100 Å in diameter are included for comparison.

the particle actually responds as if it were made entirely of the coating material.

We have applied our expression (28) to a sphere with an Al core 50 Å in radius coated with a layer of Al₂O₃ 5 Å thick (Fig. 1), and a 50-Å core of this oxide coated with a 5-Å layer of tin (Fig. 2). Frequencies well spread in the range $0 < \omega < 1.3\omega_p$ are represented. We used the Lindhard-Mermin (LM) dielectric function for the metal.³¹ It includes bulk plasmons as well as electron-hole pair excitations. Examples where the Drude (D) local dielectric function is used are included for comparison. For the oxide we used the form appropriate to the amorphous phase,

$$\epsilon(\omega) = \epsilon_\infty + \frac{\epsilon_0 - \epsilon_\infty}{1 - \Omega(\Omega + i\Gamma)} + (1 - \epsilon_\infty) \left[1 - \frac{1}{1 - \Omega'[\Omega' + i\Gamma'(\Omega')]} \right], \quad (30)$$

where $\Omega = \omega/\omega_T$, $\Gamma = 0.322$, $\Omega' = \omega/\omega_B$, $\epsilon_0 = 5.01$, $\epsilon_\infty = 2.80$, $\hbar\omega_B = 14$ eV, $\omega_T = 706$ cm⁻¹, and $\Gamma'(\Omega') = 4[1 - \tanh(3/2\Omega')]$. It includes both the infrared bulk resonance and electronic interband transitions where for the latter an envelope function was fitted to the experimental data.^{32,33} Figure 1 shows little structure in the l -dependence of the polarizability except in the intermediate frequency range in which the strong surface plasmon in the metal dominates. Notice that two peaks are visible in Fig. 1(b), one due to the plasmon at low l and the other to electron-hole pairs. The latter is entirely absent from the Drude (labeled D) result, as expected. At low and high frequencies the coating resonances overwhelm the metal response. Also, at high values of l the particle behaves as a pure-oxide sphere and its response follows Eq. (29). We have included the pure-oxide polarizabilities for comparison (labeled OX). For the very thin oxide coating we have used in this example the crossover occurs at the rather large value of $l \sim 25$ but this number decreases for thicker layers. A similar situation occurs for the metal-over-oxide case, shown in Fig. 2. Again the polarizability does not show much structure and follows the pure-metal response at large l -values. Here the pure metal curve is included for comparison (labeled M). Note that the bulk-plasmon structure at $\omega > \omega_p$ [Fig. 2(d)] is smoothed out by the presence of the oxide core.

III. OPTICAL ABSORPTION

In the long-wavelength limit the absorption of electromagnetic energy by small particles is due mainly to the coupling of the electromagnetic field to the induced electric and magnetic dipoles. The absorption cross section is³⁴

$$\sigma_a = \frac{4\pi\omega}{c} \text{Im}(\alpha_1^{(e)} + \alpha_1^{(m)}), \quad (31)$$

where $\alpha_1^{(e)}$ and $\alpha_1^{(m)}$ are the electric and magnetic dipole polarizabilities, respectively. For typical metals at room temperature this expression is valid in the infrared region of the spectrum and below. Within this range of validity, a low ($\delta \gg a$) and a high ($\delta \ll a$) frequency regimes can

be distinguished in the magnetic term, depending on the values of the skin depth $\delta = c/\sqrt{2\pi\sigma\omega}$, with σ the conductivity of the metal, and the metal particle radius a . In the far-infrared region a metallic spherical particle 100 Å in radius satisfies the condition $\delta \gg a$ and assumes a linear dependence in ω , while a 1000-Å radius particle satisfies $\delta \ll a$ (except at frequencies below 5 cm^{-1} , where the transition region is located) and $\alpha_1^{(m)}$ assumes an $\omega^{1/2}$ dependence. For metal particles of radii greater than about 50 Å, the magnetic contribution to the far absorption cross section becomes greater than the electric contribution,³⁵ nevertheless the existence of an oxide coating on the particles increases considerably the electric dipole absorption while it almost does not affect the magnetic dipole contribution.³⁶ In what follows we shall ignore the latter.

There are three frequency regions where the presence

of an oxide coating over a metal sphere modifies significantly the response of a pure metal sphere. One is the low-frequency region where the oxide exhibits a bulk resonance ($\omega \sim \omega_T$), another is the region where the surface plasmon is excited in the metal ($\omega \sim \omega_p$), and the last one is the high-frequency region where interband transitions may take place in the oxide ($\omega \sim \omega_B$). An interesting result in the limit of very low frequencies ($\omega < 0.32\omega_T$) is that the electric multipolar polarizability of a metal sphere covered by an oxide layer is independent of the dielectric function of the metal and therefore the electric absorption cross section is completely dominated by the behavior of the dielectric coating at such frequencies. Ignoring the last term in the dielectric function (30) the following approximate expression is obtained for the electric dipole absorption cross section in such a limit,

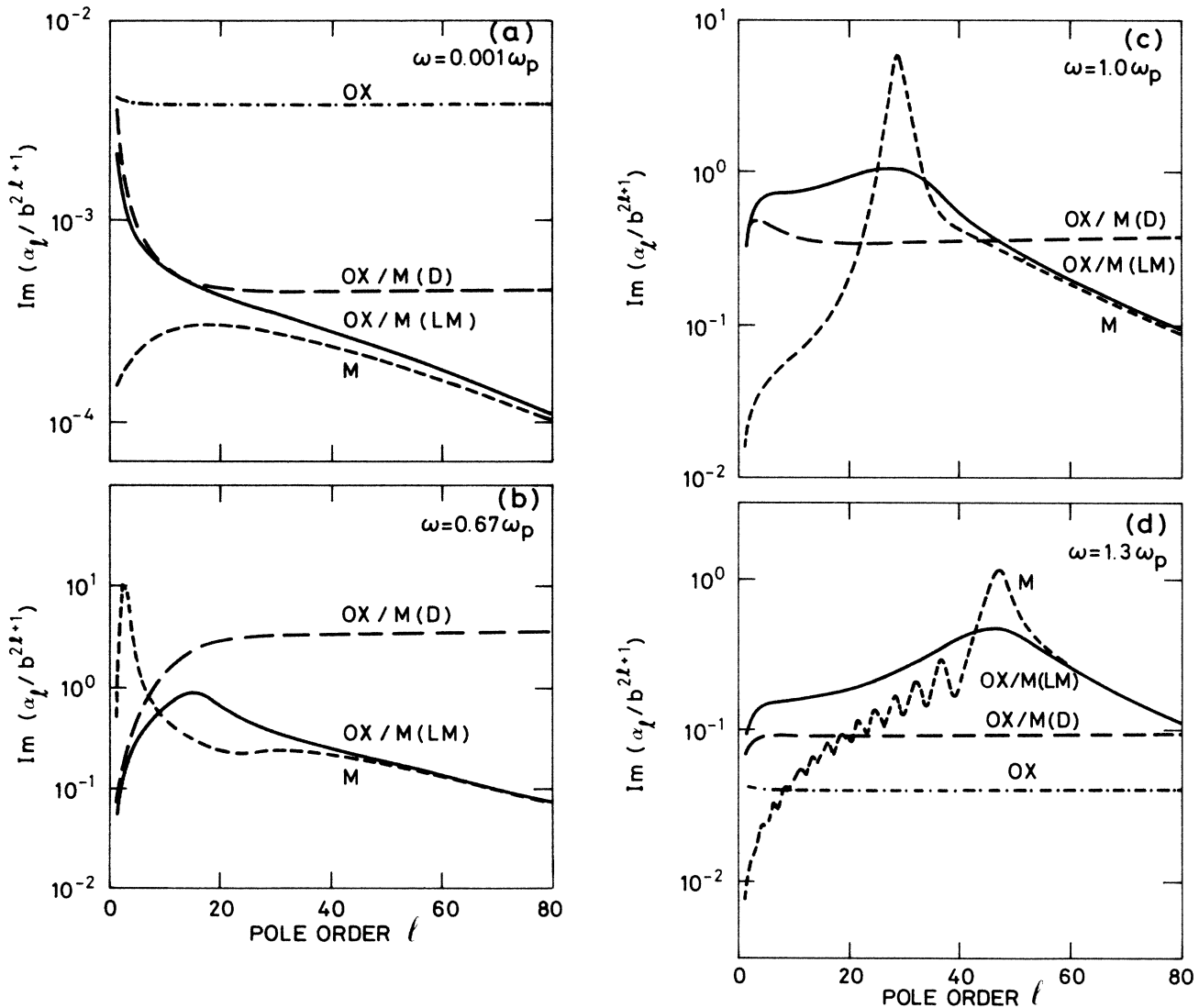


FIG. 2. Same as Fig. 1 but for an Al_2O_3 core covered by a layer of tin of same dimensions. The pure metal sphere is also included for comparison.

$$\sigma^{(e)} = \frac{12\pi}{c} \gamma b^3 \epsilon_h (\epsilon_0 - \epsilon_\infty) \frac{I_1}{(\epsilon_0 + 2\epsilon_h I_1)^2} \Omega^2, \quad (32a)$$

where

$$I_l = \frac{1 - x_l}{1 + (l+1)x_l/l}, \quad (32b)$$

$$x_l = (a/b)^{2l+1}. \quad (32c)$$

with $\gamma = \Gamma\omega_T$. For very thin layers the above relation is linear in the width $t = b - a$ of the coating.³⁷

We have obtained numerical results for the electric dipole absorption cross section of coated (σ_c) and uncoated (σ_u) spheres. In Fig. 3 we show the ratio σ_c/σ_u as a function of the relative width t of the coating for an Al/Al₂O₃ sphere of external radius 100 Å at the frequency where the phonon absorption peak due to the oxide appears, a value that varies slightly around $0.0072\omega_p$, or equivalently around $1.27\omega_T$ as a function of thickness t . We find that very thin oxide layers increase absorption by factors of 10^1 or 10^2 depending on frequency, while thicker layers give factors about one order of magnitude bigger, in agreement with earlier results.¹⁰ Because the presence of the metal is not important in this region the nonlocal character of the core dielectric function has no effect at this frequency.

Figure 4 shows the absorption cross section of an Al core 50 Å in radius with a 5-Å-thick Al₂O₃ coating (solid line) and a pure Al particle of radius 55 Å (dashed-dotted

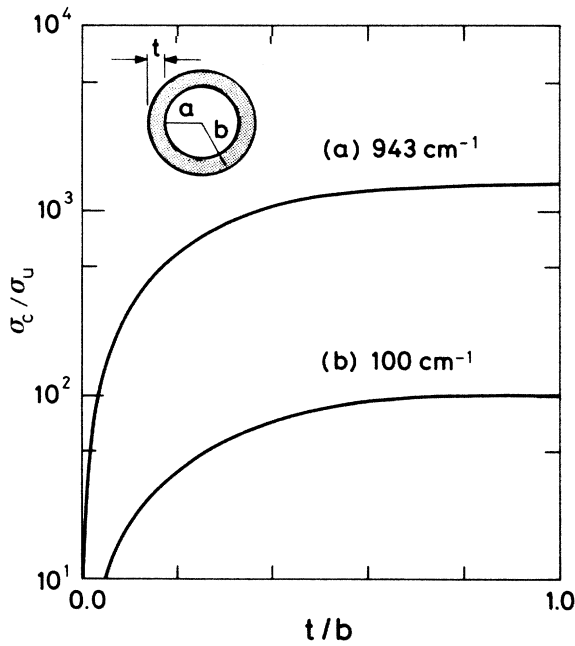


FIG. 3. Absorption cross section of an Al₂O₃-coated Al sphere of 200 Å external diameter relative to that of an uncoated sphere of the same size. t is the coating thickness. Curve (a) is for a frequency of 943 cm^{-1} , a value close to the phonon absorption peak in the oxide. Curve (b) corresponds to a far-infrared frequency of 100 cm^{-1} .

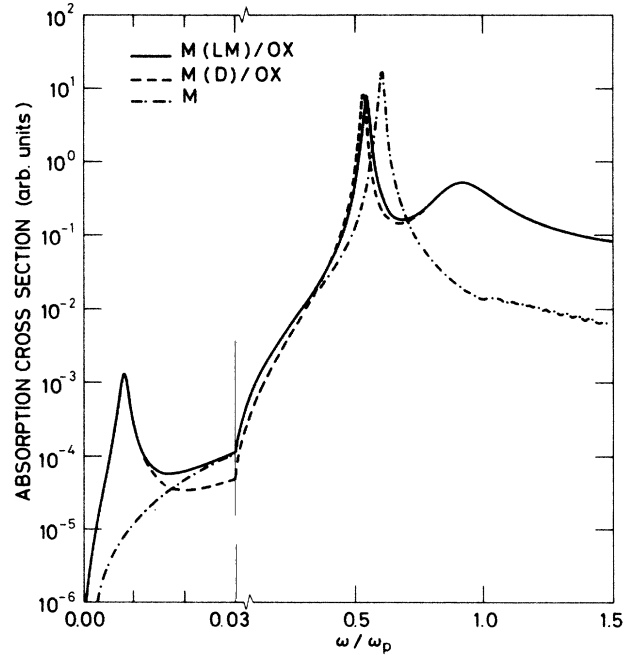


FIG. 4. Absorption cross section of an Al sphere of radius 50 Å with a 5-Å Al₂O₃ coating (solid line), and a pure Al sphere of the same external diameter (dashed-dotted line). Labels are as in Fig. 1.

line), both computed using a Lindhard-Mermin dielectric function for the metal. A third curve in Fig. 4 provides the local results obtained with a Drude model (dashed line). Inspection of this figure shows three main effects of the thin coating added to the metal core: a large enhancement and resonance in the low frequency already discussed in connection with Fig. 3, an enhancement and broad resonance at large frequencies due to interband transitions in the oxide, and finally a red shift of the surface plasmon resonance in the metal. Nonlocal effects are present through an enhancement by about a factor of 2 beyond the oxide infrared peak at low frequencies and through the small blue shift in the plasmon resonance. The approximate position of this resonance may be obtained in the local case by solving for the minima in the denominator of Eq. (28). Ignoring damping they are given by

$$\epsilon_{a,l}^*(\omega) = -\frac{l+1}{l} \epsilon_b(\omega) G_l(a, b, \omega), \quad (33a)$$

where

$$G_l(a, b, \omega) = \frac{1 - T_l(\omega)x_l}{1 + \frac{l+1}{l} T_l(\omega)x_l}, \quad (33b)$$

and

$$T_l(\omega) = \frac{\epsilon_b(\omega) - \epsilon_h}{\epsilon_b(\omega) + \frac{l+1}{l} \epsilon_h}. \quad (33c)$$

Using a Drude model for $\epsilon_a(\omega)$ and assuming that $\epsilon_b(\omega)$

is a constant over the frequency range considered, we obtain

$$\omega_l^* = \frac{\omega_p}{(1 - \epsilon_{a,l}^*)^{1/2}}. \quad (33d)$$

This relation is in agreement with that given by Munnix and Schmeitz for the limit case of very large l .³⁸ Resonances are shifted to the red by the oxide coating. If $\epsilon_b(\omega)$ is not a constant near ω_l^* , Eq. (33d) must still be solved self-consistently for ω_l^* in order to obtain the desired resonances.

Figure 5 shows the absorption cross section of an Al_2O_3 core 50 Å in radius covered by a 5-Å-thick tin layer. This case shows a plasmon resonance associated with each of the metal surfaces. A good estimate for their position may be obtained again in the zero-damping limit by solving the corresponding normal modes equation given by setting the denominator of Eq. (28) to zero. Two types of solutions emerge:

$$\epsilon_{b,l}^* = -\frac{1}{2}H_l \pm (\frac{1}{4}H_l^2 - \epsilon_a \epsilon_h)^{1/2}, \quad (34a)$$

where

$$H_l = \frac{l}{l+1} \epsilon_a + \frac{l+1}{l} \epsilon_h + (\epsilon_a + \epsilon_h)x_l, \quad (34b)$$

with x_l as given in Eqs. (32c). Solutions corresponding to the plus (minus) sign are resonances of the external (internal) surface of the metallic shell. In the $x_l \rightarrow 0$ limit the external surface solutions are given by $\epsilon_{b,l}^* = -\epsilon_a(l+1)/l$ and they correspond to a physical situation with $a=0$. In the same limit the internal surface solutions are $\epsilon_{b,l}^* = -\epsilon_a l/(l+1)$ and they correspond to a physical situation with $b \rightarrow \infty$. In Fig. 5 the two resonances are clearly visible at either side of $\omega \sim \omega_p/2$. We chose to use

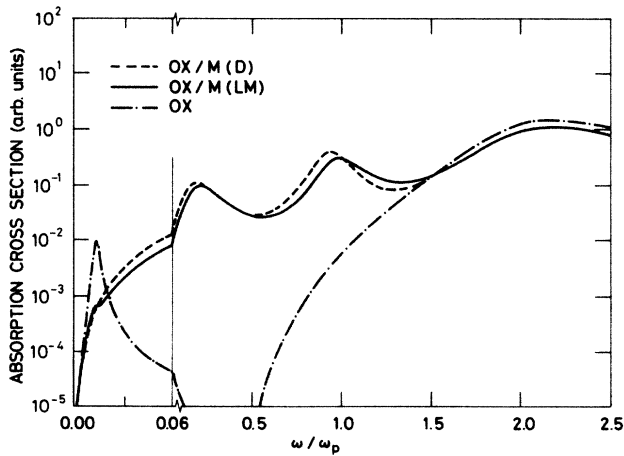


FIG. 5. Same as Fig. 4 but for an Al_2O_3 core covered by a layer of pure Al metal of same dimensions and a pure Al_2O_3 sphere.

a layer of tin metal instead of aluminum in order to avoid an overlap of the interband transitions with the inner surface plasmon peak. Figure 5 also includes the absorption cross section of a pure oxide sphere of the same external diameter for comparison (labeled OX). Strong absorption by the oxide is present at very low and high frequencies, while the metal dominates the central region as was the case for the oxide-on-metal sphere. Notice, however, that the low-frequency oxide peak is absent entirely for a Drude metal while a small feature still remains in the Lindhard-Mermin case. Again in this case the surface-plasmon resonances are slightly blue shifted when a nonlocal dielectric function is used. In the optical absorption by a single small sphere where only the dipole polarizability matters we find nonlocal effects to be small. For a metallic shell both the Drude and Lindhard-Mermin dielectric functions give two resonances associated with the inner and outer surfaces of the metal. A similar result was obtained by Lushnikov *et al.* using a jellium model with a random-phase approximation (RPA).³⁹ Recent work by Ekardt using the time dependent local density approximation shows the presence of only one resonance of mixed inner-outer surface character.⁴⁰ This result was obtained for a very small metal-on-metal sphere with an external radius less than 15 Å, well below the range we have considered in our work. Our nonlocal theory based on SCIB is a compromise that allows the treatment of larger particles but may give wrong results when quantum size effects are important or when a very thin metal coating covers an also metallic core.

IV. STOPPING POWER

Experiments using 50–100-keV electrons as a probe have proven useful in the study of electromagnetic excitations in small particles.⁴¹ If the electron passes close to the surface the field in the particle is highly nonuniform and excitations of pole order higher than dipole may be dominant.⁴² For instance a 50-keV electron at grazing incidence excites on a 200-Å sphere several multipoles, the octupole having the largest amplitude. A similar effect occurs when two spheres placed in an external electric field are very close to each other.^{43,44} The field excites the dipole on each particle which in turn produces a highly nonuniform potential in its vicinity, thus producing higher-order excitations whose relative amplitude depends on the separation of the spheres, peaking at the octupole when the center-to-center separation is 1% larger than the diameter.⁴⁵ Optical experiments on pairs of small particles require many pairs to be exposed and the difficulty in controlling their size and separation presently makes it preferable to use electrons in order to excite the multipoles under well-controlled conditions. The total energy loss by an electron passing near an oxide-coated sphere has been previously studied by Munnix and Schmeitz as a function of impact parameter.³⁸ Here we shall discuss the energy dependence of the interaction in relation to the excitation of surface resonances.

The probability that the electron loses an energy ω is given by⁴² (we use Hartree atomic units)

$$P(\omega) = \frac{4e^2}{\pi v^2 b^3} \sum_{l=1}^{\infty} \sum_{m=0}^l \frac{2 - \delta_{m0}}{(l+m)!(l-m)!} \times \left[\frac{\omega}{v} \right]^{2l} K_m^2 \left[\frac{\omega p}{v} \right] \text{Im}(\alpha_l). \quad (35)$$

Here p is the impact parameter, v the electron speed, δ_{m0} the Kronecker delta, and K_m is the modified Bessel function of order m . The total energy absorbed in the scattering process is obtained by integrating the energy multiplied by the above probability function. We have applied expression (35) to a pure Al and to an Al/Al₂O₃-coated sphere. Results for a 100-keV electron passing a distance $p=190$ Å from a 180-Å pure aluminum sphere (solid line), and a 125-Å sphere coated by a 55-Å layer of Al₂O₃ (dashed line) are shown in Fig. 6. The coating thickness was chosen so as to have the surface plasmon resonance at the same frequency as in Batson's experiment,⁵ keeping the external diameter of both spheres the same. The bulk oxide dielectric function we have used includes both the low-frequency resonance and the interband transitions as given by (30). For the metal we used the Lindhard-Mermin dielectric function. The pure aluminum sphere exhibits several peaks associated with the resonant excitation of the dipole, quadrupole and higher-pole modes, plus a kink several orders of magnitude smaller at the plasma frequency, a nonlocal effect. In contrast, the coated sphere shows only one prominent peak associated with a surface plasmon resonance and the overall width of the resonance is much smaller than in the pure metal case. One can understand this result by recalling that besides shifting the resonances to the red the oxide coating acts to suppress the excitations of higher order as discussed in Sec. III, so that one expects to see only the lowest-order peaks, in this case only the dipolar. In fact, if the sphere becomes large the dipolar resonance becomes weaker while the oxide inhibits the higher polar resonances and the overall energy loss of the electron will therefore be significantly decreased. Figure 7 is for an

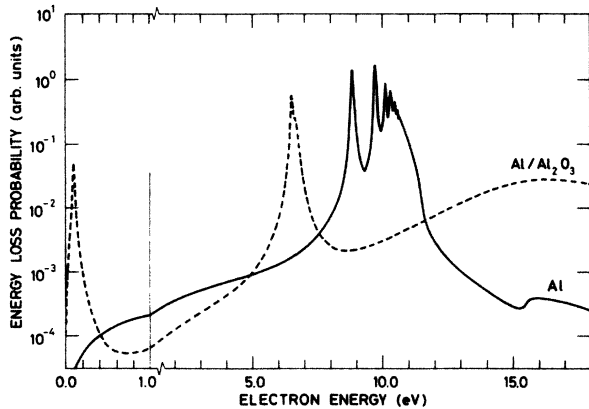


FIG. 6. Energy-loss probability function for a 100-keV electron passing 190 Å away from the center of a sphere. The latter has an Al core 125 Å in radius and a 55-Å coating of Al₂O₃ (dashed line), or is a pure Al sphere of the same external diameter (solid line).

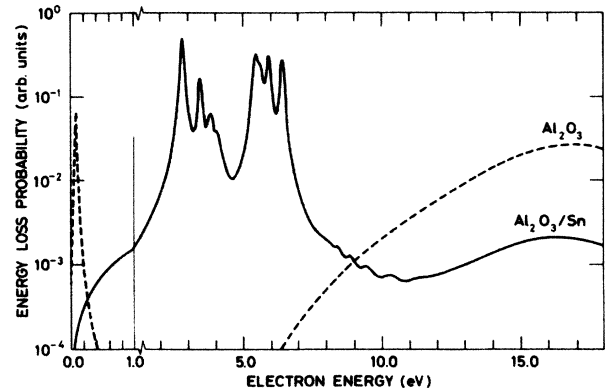


FIG. 7. Same as Fig. 6 but for an Al₂O₃ sphere with a Sn layer of same dimensions, and a pure oxide sphere.

Al₂O₃ 125-Å-radius core covered with a 55-Å layer of Sn metal (solid line), and a pure oxide sphere of the same external diameter (dashed line). Several multipoles are excited in the metallic shell and are quite visible since the coating is thick. The Mie resonance associated with the outer metal surface is the lowest frequency peak, while that associated with the inner surface is the peak of highest energy. The low-amplitude oscillations above the plasma energy are the bulk plasmon standing waves. Notice that the infrared oxide peak is entirely destroyed by the presence of the metal.

V. CONCLUSIONS

Our study of the polarizability of a coated sphere shows that for high enough pole order this quantity is dominated by the coating material, even when the latter is very thin. This effect has important consequences on the response of an oxide-coated aluminum sphere to a STEM electron, suppressing the multipolar structure in the loss probability function. Due to interband transitions the polarizability of the oxide is high in the region where the multipolar resonances occur. The same effect is expected in the optical absorption spectrum near the Mie resonance of a cluster of such spheres since, as is known, pairs of spheres or more complex arrays⁴⁶ exhibit multipolar optical resonances if the interparticle distance is less than about three particle radii. Absorption by the oxide is dominant at very low as well as very high frequencies. In the case of an oxide core coated by a metal layer the infrared oxide peak is almost entirely suppressed and two plasmon peaks occur, as an excitation in the concave and the convex metal surfaces, respectively.

Using a nonlocal dielectric function to describe the response of the metal has an important effect on the l -dependent polarizability. We find that the oxide has as a general rule the effect of smoothening out the structure introduced by the excitation of bulk plasmons and electron-hole pairs. A blue shift in the plasmon peaks is always present as a nonlocal effect, however, both for a metal core covered by oxide as for a metal shell with an

oxide core. Some nonlocal enhancement is also observed in the absorption spectrum of the particle although it reaches at most a factor of 2 in the cases studied.

ACKNOWLEDGMENTS

One of the authors (F.C.) wishes to thank Dr. P. Echenique for stimulating discussions. This work was supported by the Director for Energy Research, Office of Basic Energy Sciences, by the Division of Materials Sci-

ences, U.S. Department of Energy, under Contract No. DE-AC05-84OR21400 with Martin Marietta Energy Systems, Inc., through the University of Tennessee and Oak Ridge National Laboratory, by the United Nations Program for Development, and by Dirección de Investigaciones Universidad Católica de Chile, Grant No. 22/85. Ames Laboratory is operated for the U.S. Department of Energy by Iowa State University under Contract No. W-7405-Eng-82.

- ¹G. Mie, *Ann. Phys. (N.Y.)* **25**, 377 (1908).
- ²P. F. Liao, J. G. Bergmann, D. S. Chelma, A. Wokaun, J. Melngailis, A. M. Hawryluk, and N. P. Economou, *Chem. Phys. Lett.* **82**, 355 (1981).
- ³B. K. Russell, T. L. Ferrell, V. E. Anderson, R. J. Warmack, and J. C. Mantovani (unpublished).
- ⁴F. Claro, *Phys. Rev. B* **25**, 7875 (1982).
- ⁵P. E. Batson, *Phys. Rev. Lett.* **49**, 936 (1982).
- ⁶Y. Borensztein, P. De Andres, R. Monreal, T. Lopez-Rios, and F. Flores, *Phys. Rev. B* **33**, 2828 (1986).
- ⁷J. H. Weaver, R. W. Alexander, L. Geng, R. A. Mann, and R. J. Bell, *Phys. Status Solidi A* **20**, 321 (1973).
- ⁸R. Ruppin, *Surf. Sci.* **51**, 140 (1975).
- ⁹E. Simanek, *Phys. Rev. Lett.* **38**, 1161 (1977).
- ¹⁰R. Ruppin, *Phys. Rev. B* **19**, 1318 (1979).
- ¹¹S. S. Martinos, *Phys. Rev. B* **34**, 3900 (1986).
- ¹²S. I. Lee, T. W. Noh, and J. R. Gaines, *Phys. Rev. B* **32**, 3580 (1985).
- ¹³S. I. Lee, T. W. Noh, K. Cummings, and J. R. Gaines, *Phys. Rev. Lett.* **55**, 1626 (1985).
- ¹⁴T. W. Noh, S. I. Lee, Y. Song, and J. R. Gaines, *Phys. Rev. B* **34**, 2882 (1986).
- ¹⁵W. A. Curtin and N. W. Ashcroft, *Phys. Rev. B* **31**, 3287 (1985).
- ¹⁶J. E. Inglesfield, *Surf. Sci.* **156**, 830 (1985).
- ¹⁷A. Ljungbert and S. Lundqvist, *Surf. Sci.* **156**, 839 (1985).
- ¹⁸W. Ekardt, *Phys. Rev. Lett.* **52**, 1925 (1984).
- ¹⁹W. Ekardt, *Phys. Rev. B* **31**, 6360 (1985).
- ²⁰M. J. Puska, R. M. Nieminen, and M. Manninen, *Phys. Rev. B* **31**, 3486 (1985).
- ²¹E. Zaremba and B. N. J. Persson, *Phys. Rev. B* **35**, 596 (1987).
- ²²D. E. Beck, *Phys. Rev. B* **35**, 7325 (1987).
- ²³R. Fuchs, and F. Claro, *Phys. Rev. B* **35**, 3722 (1987).
- ²⁴W. Ekardt, *Phys. Rev. B* **32**, 1961 (1985).
- ²⁵H. Faxen, *Ann. Phys. (Leipzig)* **68**, 89 (1922).
- ²⁶B. B. Dasgupta and R. Fuchs, *Phys. Rev. B* **24**, 554 (1981).
- ²⁷G. Mukhopadhyay and S. Lundqvist, *Phys. Scr.* **17**, 69 (1978).
- ²⁸This integral is obtained starting from a result given by I. S. Gradshteyn and I. M. Ryzhik in *Table of Integrals, Series and Products* (Academic, New York, 1965), p. 692, formula 6.574.
- ²⁹B. U. Felderhof, G. W. Ford, and E. G. D. Cohen, *J. Stat. Phys.* **28**, 649 (1982).
- ³⁰See, e.g., H. C. Van der Hulst, *Light Scattering by Small Particles* (Wiley, New York, 1957), Sec. 6.34.
- ³¹N. D. Mermin, *Phys. Rev. B* **1**, 2362 (1970).
- ³²E. T. Arakawa and M. W. Williams, *J. Phys. Chem. Solids* **29**, 735 (1968).
- ³³Y. T. Chu, J. B. Bates, C. W. White, and G. C. Farlow (unpublished).
- ³⁴L. D. Landau and E. M. Lifshitz, *Electrodynamics of Continuous Media* (Pergamon, New York, 1960), pp. 193 and 194 and 229–304.
- ³⁵D. Stroud and F. P. Pan, *Phys. Rev. B* **17**, 1602 (1978).
- ³⁶The magnetic polarizability has to be computed with the radius of the metallic core, ignoring the oxide thickness. See, e.g., Refs. 11 or 15.
- ³⁷P. N. Sen and D. B. Tanner, *Phys. Rev. B* **26**, 3582 (1982). See also Refs. 12, 13, and 15.
- ³⁸S. Munnix and M. Schmeitz, *Phys. Rev. B* **32**, 4192 (1985).
- ³⁹A. A. Lushnikov, V. V. Maksimenko, and A. J. Simonov, *Z. Phys. B* **27**, 321 (1977).
- ⁴⁰W. Ekardt, *Phys. Rev. B* **34**, 526 (1986).
- ⁴¹P. E. Batson, *Surf. Sci.* **156**, 720 (1985).
- ⁴²T. L. Ferrel and P. M. Echenique, *Phys. Rev. Lett.* **55**, 1526 (1985).
- ⁴³F. Claro, *Solid State Commun.* **49**, 229 (1984).
- ⁴⁴F. Claro, *Phys. Rev. B* **18**, 7058 (1978).
- ⁴⁵R. Rojas and F. Claro, *Phys. Rev. B* **34**, 3730 (1986).
- ⁴⁶F. Claro, *Phys. Rev. B* **30**, 4989 (1984); **35**, 406 (1987).

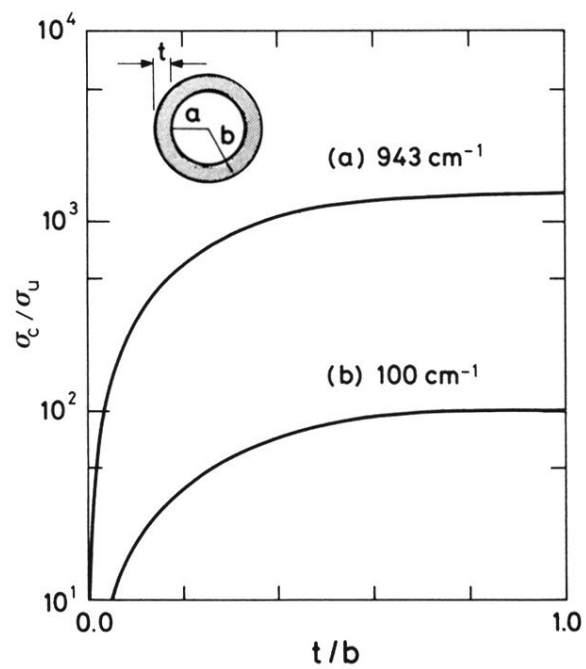


FIG. 3. Absorption cross section of an Al_2O_3 -coated Al sphere of 200 \AA external diameter relative to that of an uncoated sphere of the same size. t is the coating thickness. Curve (a) is for a frequency of 943 cm^{-1} , a value close to the phonon absorption peak in the oxide. Curve (b) corresponds to a far-infrared frequency of 100 cm^{-1} .